Grouping-Based Optimal Design of Collector System Topology for a Large-Scale Offshore Wind Farm by Improved Simulated Annealing

Ruilin Chen, Zeyu Zhang, Junxuan Hu, Lei Zhao, Chuangzhi Li, and Xiaoshun Zhang, *Member, IEEE*

***Abstract*—During the construction of an offshore wind farm (OWF), the capital cost of the collector cable system accounts for a large proportion of the total cost. Consequently, the optimal design of the collector system topology (CST) is one of the most crucial tasks in OWF planning. However, for a large-scale OWF, the optimal design of CST is a complex integer programming problem with high-dimension variables and various constraints. Therefore, it is difficult to acquire a high-quality optimal design scheme. To address this issue, this paper proposes a new grouping-based optimal design of CST for a large-scale OWF. First, all the wind turbines are divided into multiple groups according to their geographical locations and the maximum allowed connected wind turbines by each cable. This not only reduces the optimization dimension and difficulty, but also effectively satisfies the 'no cross' constraint by putting the geographically closed wind turbines into the same group. Secondly, the electrical topology among different wind turbines in each group is initially generated by an improved dynamic minimum spanning tree (DMST). The division groups of the OWF are then adjusted to further reduce the capital cost by improved simulated annealing. To verify the proposed technique, comparison case studies are carried out with five algorithms on two different OWF.**

***Index Terms*—Offshore wind farm, collector system topology, grouping-based optimal design, meta-heuristic algorithm, graph theory.**

NOMENCLATURE

A. Abbreviations

OWF	offshore wind farm
CST	collector system topology
DMST	dynamic minimum spanning tree
WT	wind turbine
MST	minimum spanning tree
GA	genetic algorithm
FCM	fuzzy *C*-means
PSO	particle swarm optimization
IA	immune algorithm
BPSO	binary particle swarm optimization
APSO	adaptive particle swarm optimization
TSP	travelling salesman problem
ACO	ant colony optimization
ISA	improved simulated annealing
EENS	expected energy not supplied
MGA	modified genetic algorithm
BIP	binary integer programming

B. Variables

f	total capital cost
C_{p}	purchase cost of the submarine cables
C_{s}	cost of shipping and installing the submarine cables
C_{f}	failure opportunity cost of CST
N_{f}	number of feeders connected to the substation
n_i	number of segments in the ith feeder
L_i^j	length of the jth segment in the ith feeder
C_i^j	cost coefficient of the jth segment in the ith feeder
K_{rw}	reliability weight of CST
E_{e}	total expected energy not supplied of the OWF
λ	efficiency coefficient
d	wind speed
V_d	wind speed distribution with d wind speed
P_v	output of the WT
F_v	wind speed frequency
P_{OWF}	installed capacity of the OWF
E_a	value of hours for the OWF out of operation
N	number of WTs
q_{L}	failure rate of submarine cables
q	failure rate of WTs
$n^{\max}$	lower bounds of the number of WTs in each feeder
$n^{\min}$	upper bounds of the number of WTs in each feeder

Received: February 28, 2023
Accepted: August 1, 2023
Published Online: January 1, 2024
Xiaoshun Zhang (corresponding author) is with the Foshan Graduate School, Northeastern University, Foshan 528311, China, and with the College of Information Science and Engineering, Northeastern University, Shenyang 110819, China (e-mail: xszhang1990@sina.cn).
DOI: 10.23919/PCMP.2023.000151

P_{t}	rated power of the substation
P_{WT}	rated power of each WT
S_{C}	maximum transmission capacity of the submarine cable
U	rated voltage of the collector system
$I_i^{\max}$	maximum current carrying capacity of the submarine cables in the *ith* feeder
$\cos\varphi$	power factor
$S_{i,j}$	capacity sum of downstream connected WTs behind the *j*th segment in the *i*th feeder
$S_{i,j}^{\max}$	maximum transmission capacity of the submarine cable for the *j*th segment in the *i*th feeder
P_i, Q_i, M_i, and N_i	location coordinates of the connected points of submarine cable
"×"	cross product
"·"	dot product
$V_{i,j}^{\min}$	minimum voltage magnitudes in each node of feeder
$V_{i,j}^{\max}$	maximum voltage magnitudes in each node of feeder
$V_{i,j}$	voltage magnitude of the *j*th node in the *i*th feeder
G	total number of WTs dividing groups
X^k	rank of WTs with each WT as starting point
X_l^k	grouping result
$F_{n_i}^k$	capital cost of grouping result
F_{DMST}	computation operation of capital cost by the DMST method
W_{n_i}	wind turbines of feeder
f_{t+1}^k	fitness value of the solution in the (*i*+1)th iteration
f_{IDMST}	computation operation of the capital cost by the improved DMST method
Z_l^m	whether the *l*th vector in $\boldsymbol{L}$ and the *m*th vector in x_t violating the no cross constraint
Δf_{t+1}	deviation of energy state between the (*t*+1) state and current best state
T	control parameter of SA in the *t*th iteration
r	length of the Markov chain
rand	a random number
K_{SA}	attenuation parameters of annealing operation

I. Introduction

In the past decade, wind energy has attracted ever increasing attention and become a hot topic in industry and academia [1]. Despite the impact of COVID-19 from 2020 to 2022, the global wind industry showed a clear sign of great resilience and a rising trend of installed capacity, with 94 GW added in 2021 [2]. From 2020 to 2021, global offshore wind energy deployment experienced a record time, with 11 879 MW of new projects commissioned, increasing from 5519 MW to 17 398 MW. In the meantime, China commissioned 13 790 MW more than the entire world had contributed up to this time [3], [4]. Based on this development trend, offshore wind energy will be one of the main energy sources in the future [5], [6].

To reduce the construction cost of an offshore wind farm (OWF), many studies have been dedicated to the optimal internal electrical and submarine cable connection system [7]. The capital cost of electrical infrastructure accounts for 15%-30% of the total initial cost of an OWF [8]. Thus, the application of optimization techniques for electrical infrastructure at the planning stage can bring obvious economic benefits [9]. Particularly, the collector system topology (CST) is the key part of the electrical infrastructure in an OWF. In general, the CST of an OWF is one of two types, i.e., radial or ring, as shown in Table I. Based on these two types, many optimization methods have been proposed for optimal design of a CST. These, are summarized below:

A. Optimization Methods for Radial Topology

Radial topology is a more economical topology than the ring since it requires shorter cable length for the wind turbine (WT) connections without any loops. For this design, the most popular methods are designed based on the minimum spanning tree (MST), genetic algorithm (GA), fuzzy C-means (FCM), K-means clustering, and particle swarm optimization (PSO). To further explore the advantages of these techniques, many methods were proposed with through the combinations of them, such as GA & MST, MST & FCM, and K-means clustering & MST. These, which can be divided into the following three categories, as follows:

1) Graph Theory Based Methods

These methods can directly generate the topology based on graph theory. The most frequently-used methods include MST and the dynamic minimum spanning tree (DMST). For the design of CST, MST can effectively reduce the required length of connected cables. However, it easily deviates from the minimization of capital cost because of the cost difference between different cables. To solve this problem, the DMST is proposed by further taking the cost weights of different cables into account [10]. Both MST and DMST can rapidly generate a feasible design solution for CST, but easily lead to high capital cost for a large-scale OWF without combination with other global optimization methods.

2) Meta-heuristic Optimization Methods

These methods can be flexibly applied to the optimal design of a CST because of their high independence on the optimization mathematical model. In [11]–[13], three variations of GA are proposed for the optimal design of a CST. Although they can easily address the

high-dimension optimization of a CST for a large-scale OWF, they can also easily be trapped into a premature convergence and violate the cross constraint [12]. For example, an improved GA is proposed in [13] for the specific case of CST by converting the optimization as a classical multiple traveling salesman problem, but it cannot satisfy the cross constraint [13] for a large-scale OWF. In [14], a binary GA is employed to determine the optimal group division for all WTs, and the connected topology of each group can be rapidly generated from MST. Similar to the MST in [14], DMST is also combined with a GA [15] to improve the optimum quality of the CST, so the capital cost can be further reduced. The optimization performance of the GA can be improved via a proper operation combined with other meta-heuristic algorithms, e.g., the combination between the cross-operators of the GA and the vaccine extraction immune algorithm (IA) [16]. As another classical meta-heuristic optimization method, different variations of PSO [17]–[19] are also proposed for the optimal design of CST due to its obvious advantages of global search and parallel calculation. In [18], the case studies show that the PSO (BPSO) can acquire a lower capital cost within the shorter convergence time than the non-dominated sorting genetic algorithm-III. In [19], an adaptive PSO (APSO) with MST is proposed to enhance the optimization ability for the optimal design of a CST. Based on the high similarity between travelling salesman problem (TSP) and the optimal design of a CST, the ant colony optimization (ACO) [20] is adopted to handle the optimal design of the CST with various constraints. To further improve optimization efficiency, MST is also combined with ACO [21] to achieve an effective reduction of optimization dimension.

TABLE I
OVERALL SUMMARY OF EXISTING OPTIMIZATION ALGORITHMS FOR THE RADIAL AND RING TOPOLOGIES

Topology	Algorithm	Number of WTs	Stability	Complexity	Computation Cost	Optimization dimension	Solution quality
Radial topology	DMST [10]	80	High	Low	Low	Low	Low
	GA [11]	280	Low	Low	Low	Medium	Low
	GA [12]	60	Low	Low	Low	Low	Low
	GA [13]	36, 64, 100, 280	Medium	Low	Low	Medium	Low
	GA & MST [14]	80	Medium	Medium	Low	Medium	Medium
	GA & DMST [15]	60	Medium	Medium	Medium	Medium	Medium
	GA & IA [16]	50	Medium	Medium	High	Medium	High
	IPSO [17]	80	Low	Low	Low	Low	Low
	BPSO [18]	78, 75, 73, 75, 70, 70, 80	Medium	Low	Low	Low	Low
	APSO & MST [19]	80	Medium	Medium	Medium	Low	Low
	ACO [20]	30	Low	Low	Low	Low	Low
	ACO & MST [21]	25	Low	Low	Low	Low	Low
	FCM [22]	626	High	Low	Low	High	Low
	DMST & FCM [23]	100	High	Low	Low	Medium	Low
	FCM & BIP & MST [24]	40	Medium	High	Medium	High	Medium
	FCM&GA&DMST [25]	112	Medium	High	High	High	High
	Clark and wright saving algorithm & MST & FCM [26]	96, 102	Medium	High	High	High	Medium
	K-means clustering & MST [27]	66	Medium	Low	Low	Low	Low
	K-means clustering & MST & firefly algorithm [28]	40	Medium	High	Medium	High	Medium
	K-clustering & MST & local search method [29]	20	High	High	High	High	High
Ring topology	ACO [20]	30	Low	Low	Low	Low	Low
	Clark and wright saving algorithm & MST & FCM [26]	96, 102	Medium	High	High	High	Medium
	FCM & GA [30]	259	Medium	Medium	Medium	High	Medium
	Clark and wright saving algorithm & PSO [31]	40	Low	High	High	Medium	Medium
	Clark and wright saving algorithm & GA & FCM [32]	160	High	High	High	High	High

3) Clustering Based Methods

For a large-scale OWF, the clustering based methods can dramatically simplify the optimization dimension by dividing the large numbers of WTs into several groups. So far, the most frequently-used clustering methods are the FCM and K-means clustering. In [22], a low complexity method based on FCM is proposed to directly acquire a feasible design solution, but the obtained capital cost is relatively high. To further reduce the capital cost, different optimization techniques including DMST [23], binary integer programming [24], DMST and GA [25], the Clark and Wright saving algorithm [26], have been combined with FCM. Similarly, the K-means clustering is often not used alone for optimal design of CST. In [27], the K-means clustering is used to group the WTs, and then MST can directly generate the topology for each group. Based on the optimization framework of K-means clustering and MST, the firefly

algorithm [28] and the local search method [29] are designed to further improve the topology quality and reduce the capital cost of CST.

B. Optimization Methods for Ring Topology

Compared with the radial topology, the ring topology is a more reliable topology with loop connections from WTs to substations. However, the design complexity of the ring topology is higher, as is the capital cost. ACO [20] and improved FCM [26] can be applied to both the radial topology and ring topology. In [30], the ring topology is decomposed into a substation layer, a WT layer, and a submarine cable layer, then the FCM and GA are combined to solve this hierarchical optimization of CST [30]. In [31], the optimal location of each substation can be obtained by PSO, and the optimal connections between different WTs are acquired by a two-phase Clark and wright saving algorithm. In order to improve the solution quality, the Clark and wright saving algorithm is combined with FCM and GA to enhance the ability of clustering and searching, respectively [32].

In summary, the ring topology based on fixed layout can provide higher operational reliability for CST, but it leads to higher capital cost [33]. Generally, the power system of an OWF contains dozens or hundreds of WTs [34]. However, the failure probability of a buried undersea cable is quite low, and is about 0.015 occ/(km·year). Consequently, the radial topology with a lower capital cost has become a popular way for CST in OWF. As the existing studies show in Table I, it is difficult to acquire high-quality design solutions of a CST for large-scale OWF by only using a single method. Although, the graph theory-based methods can rapidly generate feasible design solutions for a CST, they can easily result in high capital cost, especially for a large-scale OWF with large numbers of WTs. In addition, while the meta-heuristic optimization methods have excellent characteristic on the global exploration and model-free optimization, they are difficult to handle the CST design with multiple constraints and high-dimension variables. Finally, although the clustering based methods can dramatically reduce optimization dimension and difficulty by dividing the large numbers of WTs into several groups, it is hard to generate high-quality design solutions due to its weak ability of global exploration. Hence, the combination of these methods is more suitable for the optimal design of CST through effectively integrating their advantage. Consequently, this paper proposes a new hybrid method based on graph theory, the meta-heuristic optimization, and a grouping-based method. Compared with the existing studies, the main novelties of this work can be summarized as:

1) The proposed grouping strategy can fully consider the maximum cable transmission capacity, the installed capacity of each WT, and the locations of WTs with the substation as the coordinate origin. As a result, it can effectively avoid violating the cable transmission capacity and no cross constraints in advance, thus an efficient optimization can be implemented without these strong constraints based on the grouping results.

2) An improved DMST is proposed to rapidly generate the electrical topology among different WTs in each group, while the division groups will be adjusted by an improved simulated annealing (ISA). Hence, a global coordinated design and a deep local exploitation can be achieved for CST, which can effectively improve optimization efficiency and optimum quality.

The rest of the paper is organized as follows. Section II provides the optimization mathematical model of the CST. In Section III, the algorithm principle and design process are introduced in detail. Section IV gives the case studies and results discussions, and conclusions are presented in Section V.

II. Mathematical Model of Collector System Topology Design

A. Objective Function

In this paper, the objective function of CST design is the minimization of capital cost, consisting of includes the purchase, shipping and installation cost of submarine cables, and is given as [13]:

$$\min f = C_{\mathrm{p}} + C_{\mathrm{s}} + C_{\mathrm{f}} \tag{1}$$

where f is the total capital cost; C_{p} is the purchase cost of the submarine cables; C_{s} is the cost of shipping and installing the submarine cables, which is set to be proportional with the length of the undersea cables; and C_{f} represents the failure opportunity cost of CST.

Note that the purchase cost C_{p} is simultaneously determined by the type and length of the undersea cables. In general, the type of undersea cables can be selected according to the transmission capacity requirement of the connected WTs. In an OWF, the total purchase cost can be calculated as [15]:

$$C_{\mathrm{p}} = \sum_{i=1}^{N_{\mathrm{f}}} \sum_{j=1}^{n_i} L_i^j C_i^j, i = 0,1,2,\cdots,N_{\mathrm{f}}; j = 0,1,2,\cdots,n_i \tag{2}$$

where N_{f} is the number of feeders connected to the substation; n_i represents the number of segments in the ith feeder; L_i^j denotes the length of the jth segment in the ith feeder; and C_i^j is the cost coefficient of the jth segment in the ith feeder.

The failure opportunity cost C_{f} is equivalent to the cost during the failure of a submarine cable which prevents WTs from generating electricity, and can be written as [35]:

$$C_{\mathrm{f}} = \pi K_{\mathrm{rw}} E_{\mathrm{e}} \tag{3}$$

$$K_{\mathrm{rw}}=\left(\lambda T\sum_{v=0}^{V_d}P_vF_v\right)/P_{\mathrm{WT}},V_d=0,1,2,\cdots,d \tag{4}$$

$$E_{\mathrm{e}}=P_{\mathrm{OWF}}E_a \tag{5}$$

$$E_a=8760\left(1-\frac{E_{\mathrm{x}}}{P_{\mathrm{OWF}}}\right) \tag{6}$$

where K_{rw} represents the reliability weight of the CST, which can be affected by wake effect and ambient temperature; E_{e} represents the total expected energy not supplied (EENS) of the OWF, which is the total amount of power outages caused by the failure of the CST in a year based on WTs being normal throughout the year [36]; λ represents the efficiency coefficient which for carefully laid out wind farms will have a typical value of 0.9–0.95; d represents the wind speed; V_d represents the wind speed distribution with d wind speed, while P_v and F_v represent the output of the WT and the wind speed frequency, respectively; P_{OWF} represents the installed capacity of the OWF; and E_a represents the value of hours for the OWF being out of operation [37].

E_{x} represents the expected value of the output power for the topology considering the failure of the CST, which can be written as:

$$E_{\mathrm{x}}=\left(1-\prod_{k=0}^{N}(1-q_{\mathrm{L}})\right)\left(\sum_{l=0}^{N}(N-l)P_{\mathrm{WT}}C_N^l q^l(1-q)^{N-l}\right) \tag{7}$$

where N represents the number of WTs; q_{L} represents the failure rate of submarine cables; and q denotes the failure rate of WTs.

B. Constraints

For the CST design, the constraints mainly include the selection constraints of undersea cable connected WTs and the undersea cable connection constraints, as described below:

1) Quantity Constraint of WTs in Each Feeder

Limited by the allowed number of feeders connected to the substation, the number of WTs of each feeder should be more than the minimum required number. In addition, the number of WTs of each feeder is limited by the maximum transmission capacity of the submarine cables. Therefore, the quantity constraint of WTs in each feeder can be described as:

$$\begin{cases} n^{\min}\leqslant n_i\leqslant n^{\max} \\ n^{\min}=\dfrac{P_{\mathrm{t}}}{n^{\max}P_{\mathrm{WT}}} \\ n^{\max}=\dfrac{S_{\mathrm{C}}}{P_{\mathrm{WT}}} \\ S_{\mathrm{C}}=\sqrt{3}UI_i^{\max}\cos\varphi \end{cases} \tag{8}$$

where $n^{\max}$ and $n^{\min}$ represent the lower and upper bounds of the number of WTs in each feeder, respectively; P_{t} is the rated power of the substation; P_{WT} denotes the rated power of each WT; S_{C} represents the maximum transmission capacity of the submarine cable; U is the rated voltage of the collector system; $I_i^{\max}$ represents the maximum current carrying capacity of the submarine cables in the ith feeder; and $\cos\varphi$ is the power factor.

2) Capacity Constraint of Submarine Cable

For each feeder, the types of submarine cables for each segment are different. Hence, the maximum transmission capacity of the submarine cable for each segment should be larger than the capacity sum of the downstream connected WTs, as [13]:

$$S_{i,j}\leqslant S_{i,j}^{\max},i=0,1,2,\cdots,N_{\mathrm{f}};j=0,1,2,\cdots,n_i \tag{9}$$

where $S_{i,j}$ denotes the capacity sum of downstream connected WTs behind the jth segment in the ith feeder; and $S_{i,j}^{\max}$ is the maximum transmission capacity of the submarine cable for the jth segment in the ith feeder.

3) No Cross Constraint of Submarine Cables

Crossing submarine cables (see Fig. 1) leads to extra expense for building one cable on the top of another, additional reactive power loss, and higher damage risk [23]. Hence, any two different submarine cables should satisfy the no cross constraint, which is employed to each segment of feeder. From the location coordinates of connected WTs, this constraint can be described as:

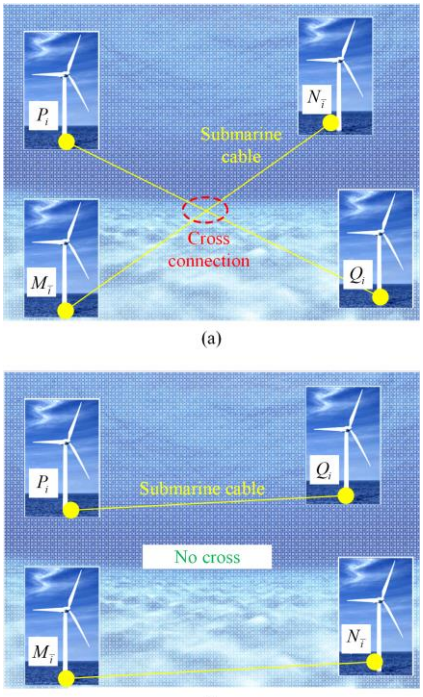

Fig. 1. Illustration of cross submarine cables. (a) Cross submarine cables. (b) No cross submarine cables.

$$\begin{cases}(M_{\bar{i}}-P_i)\times(Q_i-P_i)\cdot(N_{\bar{i}}-P_i)\times(Q_i-P_i)<0,\\ i=0,1,2,\cdots,N_{\mathrm{f}}\\ (P_i-M_{\bar{i}})\times(N_{\bar{i}}-M_{\bar{i}})\cdot(Q_i-M_{\bar{i}})\times(N_{\bar{i}}-M_{\bar{i}})<0,\\ \bar{i}\neq i\end{cases} \tag{10}$$

where P_i, Q_i, M_i, and N_i are the location coordinates of the connected points by these two submarine cables; "×" represents cross product; and "·" denotes the dot product.

4) Voltage Constraint

The voltage magnitude of each node should be limited within its lower and upper bounds, as

$$V_{i,j}^{\min}\leqslant V_{i,j}\leqslant V_{i,j}^{\max}, i=0,1,2,\cdots,N_{\mathrm{f}}; j=0,1,2,\cdots,n_i \tag{11}$$

where $V_{i,j}^{\min}$ and $V_{i,j}^{\max}$ represent the minimum and maximum voltage magnitudes in each node of the feeder, respectively; and $V_{i,j}$ represents the voltage magnitude of the *j*th node in the *i*th feeder.

III. Algorithm Principle and Design Process

Generally, the optimization method relies on a graph theory-based method, meta-heuristic algorithm, and clustering based method, and suffers from unstable results and being unable to iterate and search for a better solution of global optimization [34]. There are two main challenges in the combination of these methods. First, the optimization task of CST design need be effectively decomposed into multiple processes, so each algorithm can then be effectively implemented for each process. Secondly, the advantages of each algorithm need to be fully exploited, while their disadvantages should be avoided as much as possible. In this paper, the combination of graph theory-based method, meta-heuristic algorithm, and clustering based method is optimized to solve the CST optimization of OWF. As illustrated in Fig. 2, the proposed approach consists of two main processes.

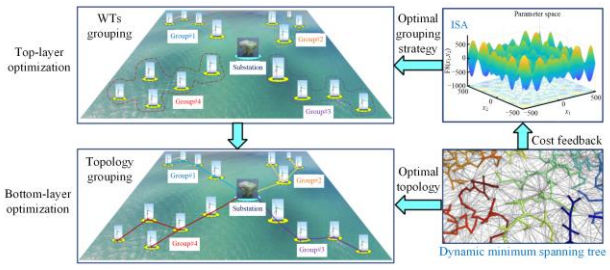

Fig. 2. Operational framework of the proposed approach for CST design.

First, a few initial need to be found to the problem solutions while satisfying all constraints. All of WTs with the same power divided into groups by polar coordinates can avoid the no cross constraint effectively. In general, each group of WTs has the same quantity to achieve power balance, and WTs are then connected group by group with an improved minimum spanning tree. This algorithm is called improved DMST, and will be introduced in the following sections**.** The layout of an OWF with large numbers of WTs is quite complex, and satisfying the no cross constraint can be difficult. However, this grouping method can generate solutions without submarine cable crossing, regardless of the complexity of the OWF. The solutions satisfying the no cross constraint with high feasibility can be the initial solutions.

Secondly comes, optimizing those initial solutions by ISA. The initial solutions are generated by dividing and connecting while grouping is only determined by polar coordinates. Therefore, it is mostly likely not the best grouping and has room for optimization. ISA can optimize initial solutions by switching WTs between groups. In this way, better grouping can be generated by ISA, while the grouping optimization schemes can be further optimized by the improved DMST.

A. Problem Decomposition

To simplify CST the problem, the original optimization problem can be decomposed into two sub-problems of initial optimization and deep optimization. The initial optimization can acquire feasible solutions, which are not economic enough for application in practical cases. Subsequently, the deep optimization process can further optimize the solutions which are produced by initial optimization to keep the capital cost as low as possible. Then each part of problem can implement a self-organizing optimization for each sub-problem.

B. Generate Initial Solutions

1) Polar Grouping

To achieve a distributed optimization for the WT connection system, WTs are ranked and divided into groups by polar coordinates with substation as the origin. Each group has same number of WTs, but the last group can be fewer in number than the general number of other groups. The quantity of WTs can be changed from $n^{\min}$ to $n^{\max}$. Each WT can be the starting point which means the quantity of WTs decides the dividing number of groups, as shown in Fig. 3. The total number of groups can be described as:

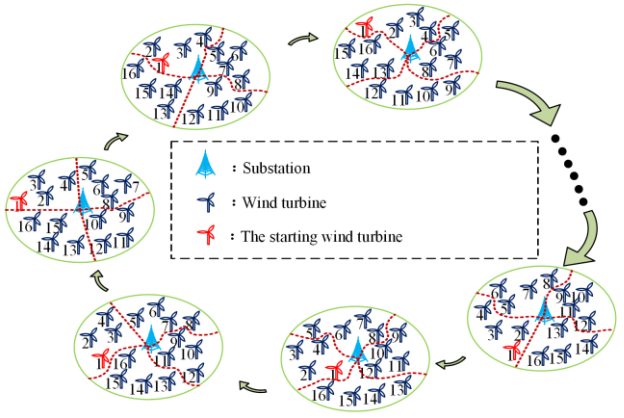

Fig. 3. Grouping traversal process.

$$G = N(n^{\max} - n^{\min} + 1) \tag{12}$$

where G denotes the total number of WTs divided in groups.

2) Intra-Group Connections

To find the best connection scheme for the single group of WTs, the optimization model applies improved DMST to optimize the intra-group connection. In a WT connection system, upstream undersea cables can be changed while adding WTs downstream. Therefore, every time WTs are added, the factor of upstream edges should be changed while calculating optimization model cost. The improved DMST is based on prim algorithm and the added factors to generate a minimum spanning tree. Modified by the prim algorithm, the improved DMST can form a directed graph and add factors to every edge to update iterations while adding each edge.

In improved DMST, two sets $\tilde{M} = \{0\}$ and $\tilde{N} = \{i \mid i \in n_l\}$ are created first to represent the set of substations and WTs, which have been connected to the tree and a set of WTs not connected to the tree, respectively. Secondly, the connection order of WTs is ranked by the distance to the substation. Thirdly, the first WT of in N is chosen and connected to each individual in $\tilde{M}$ to calculate the factor and find which connected object can be the best. Next comes adding the WT to $\tilde{M}$ and deleting from $\tilde{N}$. Additionally, a set of edge $\tilde{L} = \{\varnothing\}$ is created to save the connection relationship. The third step is then repeated for all WTs connecting to the tree until $\tilde{N} = \{\varnothing\}$ and $\tilde{M} = \{0, i \mid i \in n_l\}$. Lastly, the topology tree and the capital cost of CST are generated.

The processes of the improved DMST forming directed graph and connecting WTs are shown in Fig 4.

In this work, all WTs are assumed to be the same and there are four types of submarine cables. According to the constraints, black cable, green cable, blue cable, yellow cable can load 2, 3, 4, and 5 WTs, respectively. As shown above, every step of connecting has a corresponding cable to show the directed graph.

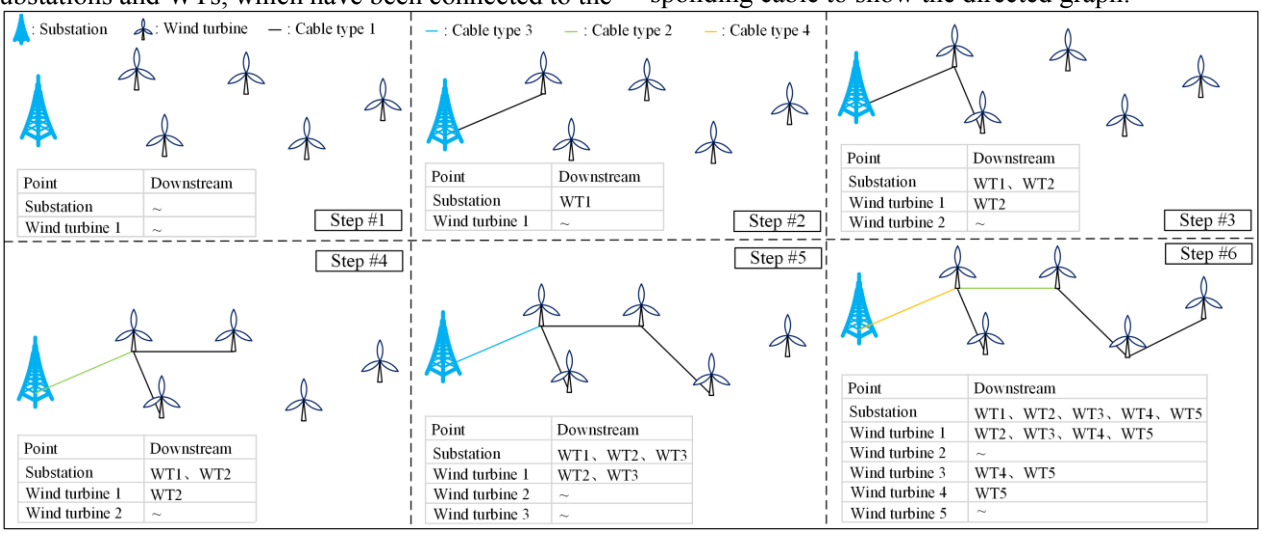

Fig. 4. The processes of improved DMST in single group.

C. Deep Optimization

In this section, ISA is proposed to solve the CST for the OWF. First, to find search the optimal result quickly, the mutation operator and the mutation operation are proposed in ISA. Secondly, in the iteration process, the memory mechanism is proposed to quickly calculate the cost function by computing the costs of the two groups in the mutation operation. Lastly, in the no cross constraint, the priority of the judgment of violation constraint is lower than computation of capital cost, because the computation of capital cost is easier and faster than the judgment of violation constraint.

1) Initialization for ISA

The maximum number of groups N_{f} and maximum number of the WTs in each group $n_i^{\max}$ are initialized according to the number of WTs. First, the preliminary solution is obtained by the polar grouping method, as:

$$X^k = [X^1, X^2, \cdots, X^N] \tag{13}$$

where X^k represents the rank of WTs with each WT as starting point.

Then, the ranks are decomposed by different numbers of WTs in one group, which can be written as:

$$X_{n_i}^k = \begin{bmatrix} X_{n^{\min}}^1, & X_{n^{\min}+1}^1, & \cdots, & X_{n^{\max}}^1 \\ X_{n^{\min}}^2, & X_{n^{\min}+1}^2, & \cdots, & X_{n^{\max}}^2 \\ \vdots & & \ddots & \vdots \\ X_{n^{\min}}^{N_{\mathrm{f}}}, & X_{n^{\min}+1}^{N_{\mathrm{f}}}, & \cdots, & X_{n^{\max}}^{N_{\mathrm{f}}} \end{bmatrix} \tag{14}$$

where X_l^k represents the grouping result.

The corresponding inter-group connection with the

capital cost can be computed by DMST, which cost can be described as:

$$F_{n_i}^k = F_{\text{DMST}}(X_{n_i}^k), k = 0,1,2,\cdots,N \tag{15}$$

where $F_{n_i}^k$ represents the capital cost of grouping result; and F_{DMST} represents the computation operation of capital cost by the DMST method.

Through the grouping method, all initial solutions can satisfy the no crossing constraint. Each epoch of ISA has one individual, and the optimal capital cost f_0 and best grouping solution x_0 can be selected from the initial solutions.

2) Mutation Operation for ISA

Generally, the new solution is obtained by the mutation operation. Two random parameters are given in the mutation operation. The two parameters p and q are given to select the two mutation wind farms in different groups. For example, the solution in the tth iteration is given as the random parameters $p = [p_1, p_2]^T$ and $x_t = \left[x_t^1, x_t^2, \cdots, x_t^{p_1}, \cdots, x_t^{p_2}, \cdots, x_t^{N_f}\right]$ to determine the selected feeders, where t represents the number of WTs. Then the random parameters $q = [q_1, q_2]^T$ determine the selected WTs, which can be represented as $x_t^{p_1} = \left[W_1, W_2, \ldots, W_{q_1}, \ldots, W_{n_i}\right]$ and $x_t^{p_2} = \left[W_1, W_2, \cdots, W_{q_2}, \cdots, W_{n_i}\right]$. The new solution in the (t+1)th iteration is given as $x_{t+1}^{p_1} = \left[W_1, W_2, \cdots, W_{q_2}, \cdots, W_{n_i}\right]$ and $x_{t+1}^{p_2} = \left[W_1, W_2, \cdots, W_{q_1}, \cdots, W_{n_i}\right]$. Particularly, if the two mutation WTs are in the same group, i.e., $p_1 = p_2$, the mutation operation will be reset.

3) Mutation Operation for ISA

After the new solutions are obtained, the improved DMST is employed to rapidly obtain the inter-group connection with the two mutation groups and combine with the other groups remaining the as same as in the previous iteration. From the two mutation groups, the algorithm only computes the cost values of the two groups. The cost values of the other groups remain unchanged, as:

$$f_{t+1}^i = \begin{cases} f_{\text{IDMST,V}}(X_{t+1}^i), \\ if\ i = p_1\ or\ i = p_2\ is\ satisfied \\ f_{t+1}^i\ , i = 1,2,\cdots,N_f \end{cases} \tag{16}$$

where f_{t+1}^k represents the fitness value of the solution in the (i+1)th iteration; and f_{IDMST} represents the computation operation of the capital cost by the improved DMST method.

Then the total fitness value should take the capital cost value and the violation of the no cross constraint into account. Through the group format, the algorithm reduces not only the cost computation of the two groups, but also the computation cost of the no cross constraint with a judgement of matrix $\boldsymbol{L}$. The connection set of the sth feeder can be given as $\boldsymbol{L} = \begin{bmatrix} x_t^{s_1} \\ x_t^{s_2} \end{bmatrix}$, which represents the set of the selected feeder. The total connection set of the OWFs can be given as $x_t = \left[x_t^1, x_t^2, \cdots, x_t^{s_1}, \cdots, x_t^{s_2}, \cdots, x_t^{N_f}\right]$. The improved DMST can judge whether the two selected feeders are crossing each other, and the judgement result matrix $\boldsymbol{Z}$ can be described as:

$$\boldsymbol{Z}_l^m = \begin{cases} 0, s.t.Eq.(6) \\ 1 \end{cases}, l = 1,2; m = 1,2,\cdots,N_f \tag{17}$$

where $\boldsymbol{Z}_l^m$ represents whether the lth vector in L and the mth vector in x_t violate the no cross constraint.

In practical application, the CST needs to be subjected to the voltage constraint. Thus, a power flow calculation will be applied in the optimization results to judge whether the CST violates the voltage constraint, and the judgement result matrix $\boldsymbol{Y}$ can be written as:

$$\boldsymbol{Y}_l^i = \begin{cases} 0, If\ Eq.(3) is\ satisfied \\ 1, Otherwise \end{cases}, l = 1,2; i = 1,2,\cdots,N_f \tag{18}$$

The fitness value can be determined by judgement matrix $\boldsymbol{Z}$, matrix $\boldsymbol{Y}$ and the capital cost, as:

$$f_{t+1}^i = \begin{cases} f_{t+1}^i + 10^{15} \times \sum_{l=1}^{2}\sum_{i=1}^{N_f}(\boldsymbol{Z}_l^i + \boldsymbol{Y}_l^i), \\ if\ i = p_1\ or\ i = p_2\ is\ satisfied \\ f_{t+1}^i\ , i = 1,2,\cdots,N_f \end{cases} \tag{19}$$

4) Annealing Operation

Through the fitness values computation, the new solution can be accepted if the Metropolis formula meet the demand, i.e.:

$$\Delta f_{t+1} = f_{t+1}^{p_1} + f_{t+1}^{p_2} - f_{\text{best}}^{p_1} - f_{\text{best}}^{p_2} \tag{20}$$

$$f_{\text{best}}^i = \begin{cases} f_{t+1}^i, s.t. \exp\left(-\frac{\Delta f_{t+1}}{T_{t+1}}\right) > rand, s.t. i = P_1, P_2 \\ f_{\text{best}}^i \end{cases} \tag{21}$$

$$X_{\text{best}}^i = \begin{cases} X_{t+1}^i, s.t. \exp\left(-\frac{\Delta f_{t+1}}{T_{t+1}}\right) > rand, i = P_1, P_2 \\ X_{\text{best}}^i \end{cases} \tag{22}$$

$$T_{t+1} = \begin{cases} K_{\text{SA}} \cdot T_t, s.t.t\ is\ the\ multiples\ of\ r \\ T_t \end{cases} \tag{23}$$

where Δf_{t+1} represents the deviation of energy state between the $(t+1)$ state and the current best state; and

$\exp\left(-\frac{\Delta f_{t+1}}{T}\right)$ is the parameter that determines whether the system receives the $(t+1)$ state's change; T is the control parameter of SA in the tth iteration; r is the length of the Markov chain; *rand* represents a random number; and K_{SA} represents the attenuation parameters of the annealing operation.

D. Execution Procedure

Overall, the specific execution procedure of ISA for the submarine cable connection system of an OWF is given in Table II.

TABLE II
THE SPECIFIC EXECUTION PROCEDURE OF ISA FOR SUBMARINE CABLE CONNECTION SYSTEM

Input: The submarine cable cost factor and coordinates of WTs;
1: Calculate the distance matrix between WTs and substation;
2: Dividing WTs into groups by polar coordinates;
3: Connecting each WTs groups by DMST;
4: Initialize the parameters and operators of ISA;
5: Initialize the groups, connections, solution and fitness value;
6: WHILE $T_t > T_{\max}$
7: Select the mutation groups and execute the mutation operation according to the random operators;
8: FOR $i = p_1, p_2$
9: FOR $j = 1$ **to** $n^{\max}$
10: Calculate the directed graph of WTs and determine the con-nection of WTs;
11: Execute the cost calculation by Eq. (8);
12: Record the solution, connections and cost function values;
13: END FOR
14: END FOR
15: Calculate the violation of cross constraints by Eq. (6) and fitness function values by Eq. (9);
16: Determine the annealing operation of current mutation solution by Eqs. (12)–(15);
17: Execute the drop of temperature operation;
18: $t = t + 1$;
19: END WHILE
Output: The optimal groups and connections of OWTs.

IV. CASE STUDY

To demonstrate the capability and application of the proposed technique, 2 OWFs with different quantities (i.e., 75, 250) and layouts of WTs are optimized using 6 algorithms. The main difference between the two testing systems is the testing model, including the location distribution of WTs, number of WTs, and types and cost coefficients of alternative submarine cables. In this paper, 4 algorithms combined with the improved DMST respectively, including GA, IA, SA, and ISA, are proposed to compare to the other two algorithms which are the modified genetic algorithm (MGA) and DMST [15], and DMST [10]. The main parameters needed in the optimization algorithms are given in Table III, with the evaluation times of Pattern 1 at 5000.

In different OWFs, the power of WTs can be different. In this paper, the 5 cases have two types of WTs with 8 MW and 8.5 MW, respectively. Consequently, different types of submarine cables should be applied to connect WTs in different OWFs.

TABLE III
MAIN PARAMETERS OF OPTIMIZATION ALGORITHMS

Algorithm	Parameter	Value
ISA	Attenuation parameters	0.99
	Initial temperature	50
	Generations	20 000
SA	Attenuation parameters	0.99
	Initial temperature	N/2
	The length of Markov chain	200
	Generations	100
IA	Immune selected ratio	1
	Population refresh ratio	0.5
	Maximum immune generation	100
	Immune population	100
	Number of clones	2
GA	Crossover probability	1
	Mutation probability	1
	Population	200
	Generations	100
MGA	Crossover probability	1
	Mutation probability	1
	Population	200
	Generations	100

Additionally, it is important to note that a true evaluation would require years of measured wind speed data [38]. For clarity, this paper applies the sample data consisting of three years of hourly wind speed data, as shown in Fig. 5, which provides the wind speed frequency distribution and cumulative frequency of this data set. In this paper, the 2 cases apply the WTs with 8 MW, so the power curve of the 8 MW WTs is provided in Fig. 6.

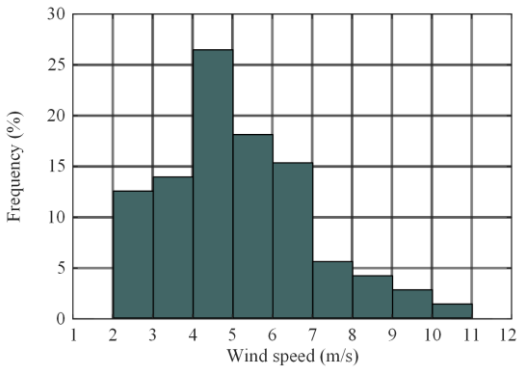

Fig. 5. Wind speed frequency distribution.

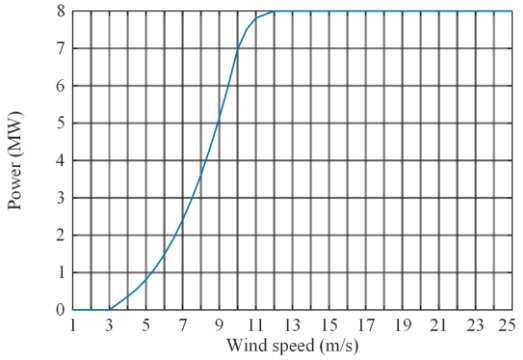

Fig. 6. Typical power curve of the 8 MW wind turbine.

The rated bus voltage is set to 66 kV, and the maximum and minimum voltages are set to 1.1 p.u. and 0.9 p.u., respectively [39].

To verify the practical implementation of the algorithms proposed to optimize the CST, 5 different experiments are conducted to evaluate the 6 algorithms. In different OWFs, the output of the submarine cable connection graph and capital cost of undersea cables are based on MATLAB R2020b. All calculations and graphing are carried out by a personal computer with Intel(R) Core i7-10700 CPU at 2.90 GHz with 8 GB of RAM.

A. Test System #1: An OWF with 75 WTs

To test the performance of the algorithms, they are applied to optimize the CST in an OWF with 75 WTs of 8 MW each, resulting in a total capacity of 600 MW. The cost of submarine cables, including equipment and construction costs, is also taken into consideration. In this study, the cable connection system consists of 3 types of submarine cables, as shown in Table IV. Based on the capacities of the submarine cables, current carrying capacities, and human intervention factors, three submarine cables are selected to connect the WTs in case 1. The cable types of #1, #2 and #3, can support up to 2, 3 and 4 WTs' current output, respectively.

TABLE IV
DATA ON SUBMARINE CABLES IN TEST SYSTEM #1

Type	Capacity (MW)	Ampacity (A)	Resistance AC 90℃ (Ω/km)	Reactance (Ω/km)	Loadable quantity of WTs	Price (￥/km×10^6/km)	Representing colour
#1	31.800	278	0.246	0.153	2	2.106	Black
#2	45.498	398	0.127	0.138	3	2.623	Green
#3	58.529	512	0.078	0.127	4	3.231	Bule

In Pattern 1, the evaluation process is conducted 20 000 times for six different methods. The optimization processes of meta-heuristic algorithms for CST are presented in Fig. 7. The number of iterations in ISA is 20 000, as every iteration only has a single individual, and the first individual is the best one of the initial groupings. The convergence process of the algorithms indicates that ISA can break through the local optimal solution. Fig. 8 shows the data of 10 runs for the meta-heuristics algorithms, including all results, mean value markers and median lines. To clarify the results of meta-algorithms, the data of DMST are shown in Table V noting that the results of deterministic algorithm are fixed values without optimization. Different from the traditional SA, the improved SA can explore the searchable space efficiently and identify the optimal solution within a specified number of iterations. In addition, there is an annealing operation, which can abandon the current solution and explore new solutions based on the suboptimal solution. Consequently, ISA can accept the suboptimal solution to expand the searchable space and prevent it from falling into a low-quality local optimum. It shows that the costs optimizing by ISA are significantly lower, indicating that ISA has greater stability and reliability to optimize the CST of an OWF. Also, it illustrates that each algorithm can find several optimal schemes for CST under this special OWF, but ISA can obtain more solutions which are better than those from other algorithms. As a result, ISA can acquire more economical schemes in the OWF for the CST problem.

In fact, the meta-heuristic optimization methods are essentially the stochastic optimization algorithm, which can easily acquire different optimal solutions in different executions. To reveal their optimization stability for the optimal design of CST, their optimization results are given with different executions. In the case studies, each meta-heuristic optimization method is executed with 10 runs for each testing system. Table V lists the lowest, average, and highest costs of submarine cable cost C_{sc} and transmission power loss cost C_o, respectively. The failure opportunity cost C_f is mostly affected by the number of WTs and the length of submarine cables.

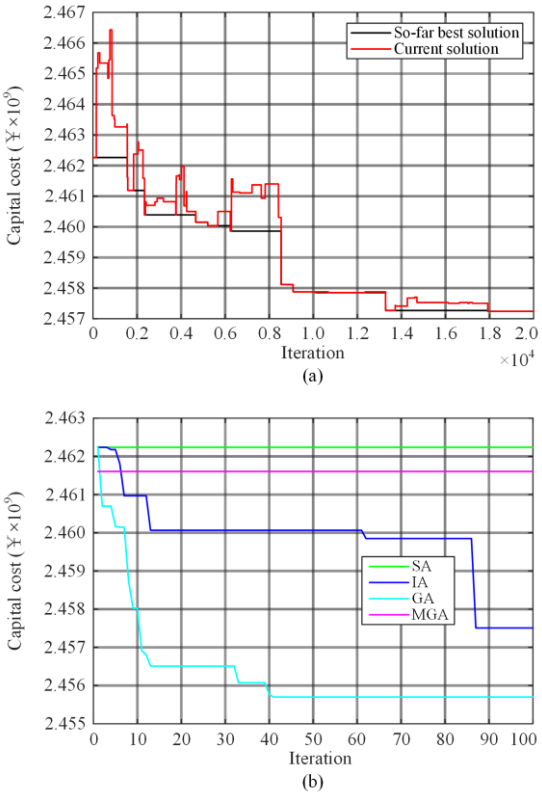

Fig. 7. The convergence process graphs of meta-heuristics algorithms for optimal design of CST in test system #1. (a) ISA. (b) SA, IA, GA & MGA.

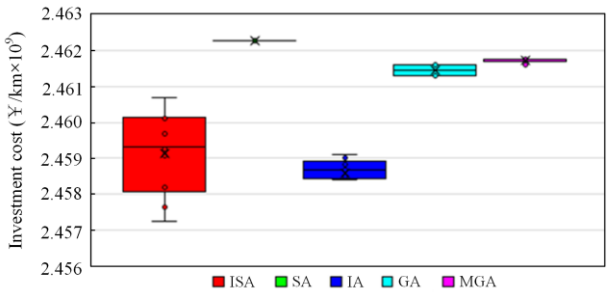

Fig. 8. The optimal costs by meta-heuristics algorithms of CST by running ten times in test system #1.

In this paper, the number of WTs is unchangeable and the change of the length of submarine cables is quite small. The failure opportunity cost is accounted over the operating cycle of the OWF i.e. 25 years. As a result, under large coefficients of the numbers of WTs and submarine cables, the effect of the length of submarine cables is further reduced. In addition, t_c^{min}, t_c^{mean}, and t_c^{max} represent the shortest, average, and longest convergence times, respectively, whereas t^{min}, t^{mean} and t^{max} represent the shortest, average, and longest computation times, respectively. It can be seen from Table V that the iteration optimization based on meta-heuristics algorithms can significantly reduce the investment costs compared a deterministic algorithm without iterating optimization. Although the computation time of the deterministic algorithm is quite low, the investment costs are higher than all meta-heuristics algorithms.

TABLE V
STATISTICAL RESULTS OBTAINED BY DIFFERENT ALGORITHMS FOR OPTIMAL DESIGN OF CST IN TEST SYSTEM #1

Algorithm		ISA	SA	IA	GA	MGA	DMST
Failure opportunity cost (¥/km×10⁹)		2.0816	2.0816	2.0816	2.0816	2.0816	2.0816
Total capital cost (¥/km×10⁹)	f_{min}	2.4572	2.4623	2.4569	2.4613	2.4616	2.4647
	f_{mean}	2.4591	2.4623	2.4586	2.4615	2.4617	2.4647
	f_{max}	2.4606	2.4623	2.4604	2.4516	2.4617	2.4647
Submarine cable cost (¥/km×10⁸)	C_{sc}^{min}	3.7564	3.8063	3.7510	3.7970	3.8001	3.8063
	C_{sc}^{mean}	3.7752	3.8063	3.7696	3.7984	3.8009	3.8063
	C_{sc}^{max}	3.7903	3.8063	3.7873	3.7998	3.8012	3.8063
Convergence time (s)	t_{min}	5.0214	4.8749	3.5109	28.3479	117.2878	3.1221
	t_{mean}	9.6960	5.0219	36.6338	65.0413	164.1541	3.2715
	t_{max}	12.9031	5.3237	84.7601	77.8860	246.0465	4.2443
Computation time (s)	t_{min}^{c}	12.5726	480.1561	6.8332	826.5699	3733.8716	3.1221
	t_{mean}^{c}	12.9050	496.8612	83.2984	1032.1911	4245.1385	3.2715
	t_{max}^{c}	13.9548	515.2403	88.5295	1283.6421	4494.1805	4.2443

Additionally, the layout of WTs and optimal CST graphs derived by ISA for the OWF is shown in Fig. 9. The CST graphs of comparison algorithms are shown in Figs. A1–A5 in the Appendix A. In a case where the WT node voltages violate the voltage constraint, the simulation applies the max wind speed of 12 m/s while the WTs generate the rated power, as shown in Figs. 5 and 6. Figure 10 shows the simulation result of the WT nodes voltage for the OWF in the proposed wind speed frequency distribution. It can be seen that the computation time of ISA is the lowest of the five meta-heuristics algorithms. By integrating the computation time and capital cost obtained by all methods, ISA can acquire high-quality solutions of the CST problem in OWF. Consequently, ISA is superior to other meta-heuristics algorithms and deterministic algorithms for OWF.

B. Test System #2: An OWF with 250 WTs

To test the robustness of the proposed ISA, Pattern 2 is employed to apply algorithms to optimize the CST of an OWF with 250 WTs and a total capacity of 2000 MW. In this study, the cable connection system consists of 6 types of submarine cables, as shown in Table VI. The cable specifications used in the benchmark are listed in Table 10 [31]. Based on the rated voltage and power, cables #1, #2, #3, #4, #5 and #6, can each withstand the current output of up to 3, 4, 5, 6, 7 and 8 WTs, respectively.

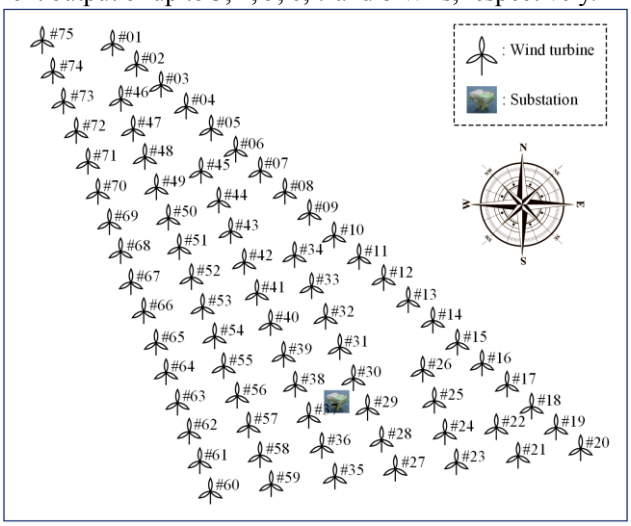

(a)

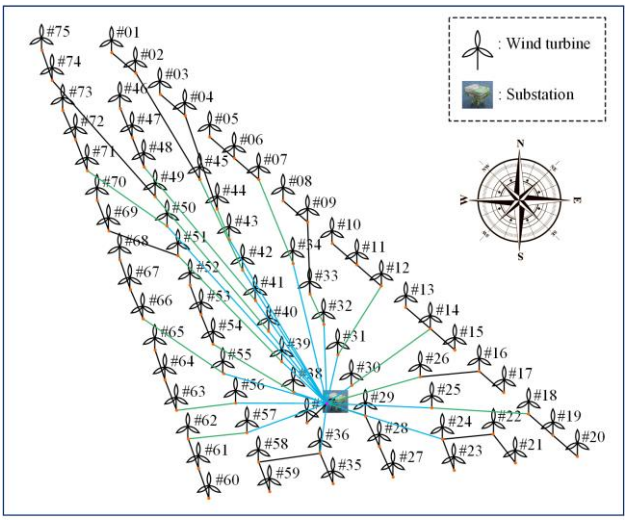

(b)

Fig. 9. The wind turbine connection graphs obtained by ISA for optimal design of CST in test system #1. (a) OWF layout. (b) ISA.

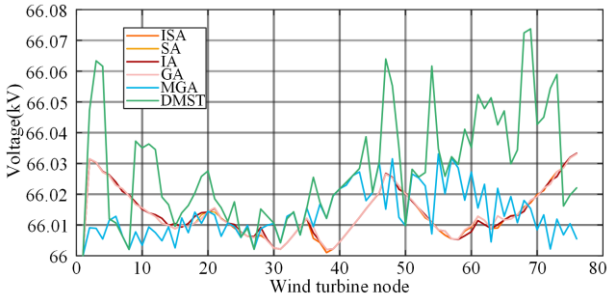

Fig. 10. The wind turbine node voltage of different algorithms for optimal design of CST in test system #1.

Similarly, Fig. 11 provides the optimization processes obtained by the six optimization algorithms for the CST problem in Pattern 2. Among the algorithms, ISA and IA stand out for their breakthrough of the local optimal and optimizing better solutions, as demonstrated in Fig. 12. As shown in Table VII, the total capital cost of the CST derived by ISA is the lowest of among all the algorithms, while the computation cost, convergence time and mean value obtained by ISA are the lowest in the meta-heuristic algorithms. Given the size of this wind farm, the computation cost of the CST is particularly important, and ISA is able to achieve fast calculation speed comparable to the other optimization algorithms. This highlights the high efficiency of ISA as an adaptive algorithm for large OWF to optimize the CST for lower total capital cost. The layout of WTs and the optimal CST graphs optimized by ISA are illustrated in Fig. 13. The optimal CST graphs are shown in Figs. A6–A10 in Appendix A. In addition, the simulation result of the WT node voltage for the OWF in the proposed wind speed frequency distribution is shown in Fig. 14.

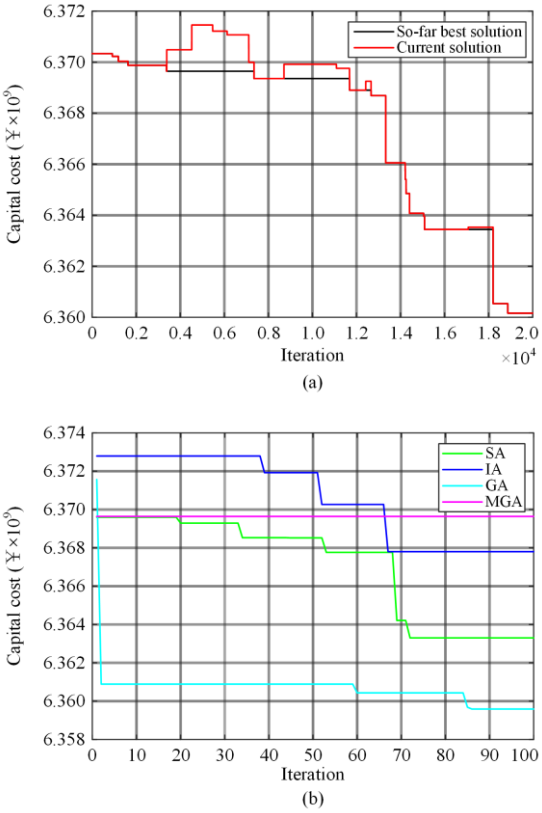

Fig. 11. The convergence process graphs of meta-heuristics algorithms for optimal design of CST in test system #2. (a) ISA. (b) SA, IA, GA & MGA.

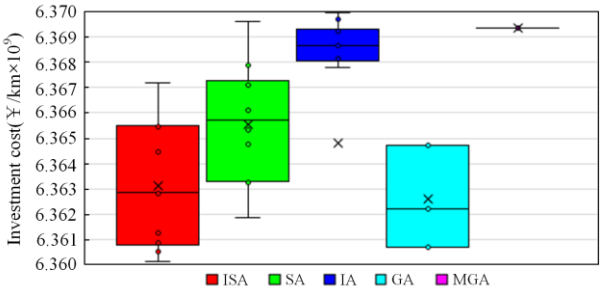

Fig. 12. The optimal costs by meta-heuristics algorithms of CST by running ten times in test system #2.

TABLE VI
DATA ON SUBMARINE CABLES IN TEST SYSTEM #2

Type	Capacity (MW)	Ampacity (A)	Resistance AC 90℃ (Ω/km)	Reactance (Ω/km)	Loadable quantity of WTs	Price (¥/km×10⁶/km)	Representing colour
#1	26.293	230	0.342	0.160	3	0.195	Black
#2	31.800	278	0.246	0.153	4	0.211	Green
#3	45.498	398	0.127	0.138	5	0.262	Bule
#4	58.592	512	0.078	0.127	6	0.323	Magenta
#5	73.390	642	0.046	0.118	7	0.421	Red
#6	90.195	789	0.027	0.112	8	0.580	Yellow

TABLE VII
STATISTICAL RESULTS OBTAINED BY DIFFERENT ALGORITHMS FOR OPTIMAL DESIGN OF CST IN TEST SYSTEM #2

Algorithm		ISA	SA	IA	GA	MGA	DMST
Failure opportunity cost (¥/km×10^9)		5.1961	5.1961	5.1961	5.1961	5.1961	5.1961
Total capital cost (¥/km×10^9)	f_{min}	6.3601	6.3633	6.3721	6.3670	6.3694	6.3696
	f_{mean}	6.3631	6.3655	6.3692	6.3626	6.3694	6.3696
	f_{max}	6.3672	6.3695	6.3696	6.3647	6.3694	6.3696
Submarine cable cost (¥/km×10^9)	C_{sc}^{min}	1.1641	1.1658	1.1717	1.1638	1.1732	1.1735
	C_{sc}^{mean}	1.1677	1.1695	1.1733	1.1665	1.1732	1.1735
	C_{sc}^{max}	1.1714	1.1718	1.1756	1.1687	1.1732	1.1735
Convergence time (s)	t_{min}^{c}	8.3643	64.707 2	158.0615	2750.4416	2808.3766	71.556
	t_{mean}^{c}	62.4668	2894.772 3	523.8322	3182.1433	4192.0756	78.0011
	t_{max}^{c}	80.7408	4541.033 1	873.4844	3762.8948	6268.8354	82.2138
Computation time (s)	t_{min}	67.7985	2695.993 7	708.5005	5252.5243	20283.900	71.556
	t_{mean}	74.8730	4146.505 5	779.5425	5720.0190	21332.343	78.0011
	t_{max}	86.5634	5472.607 6	933.9494	6998.9384	26151.193	82.2138

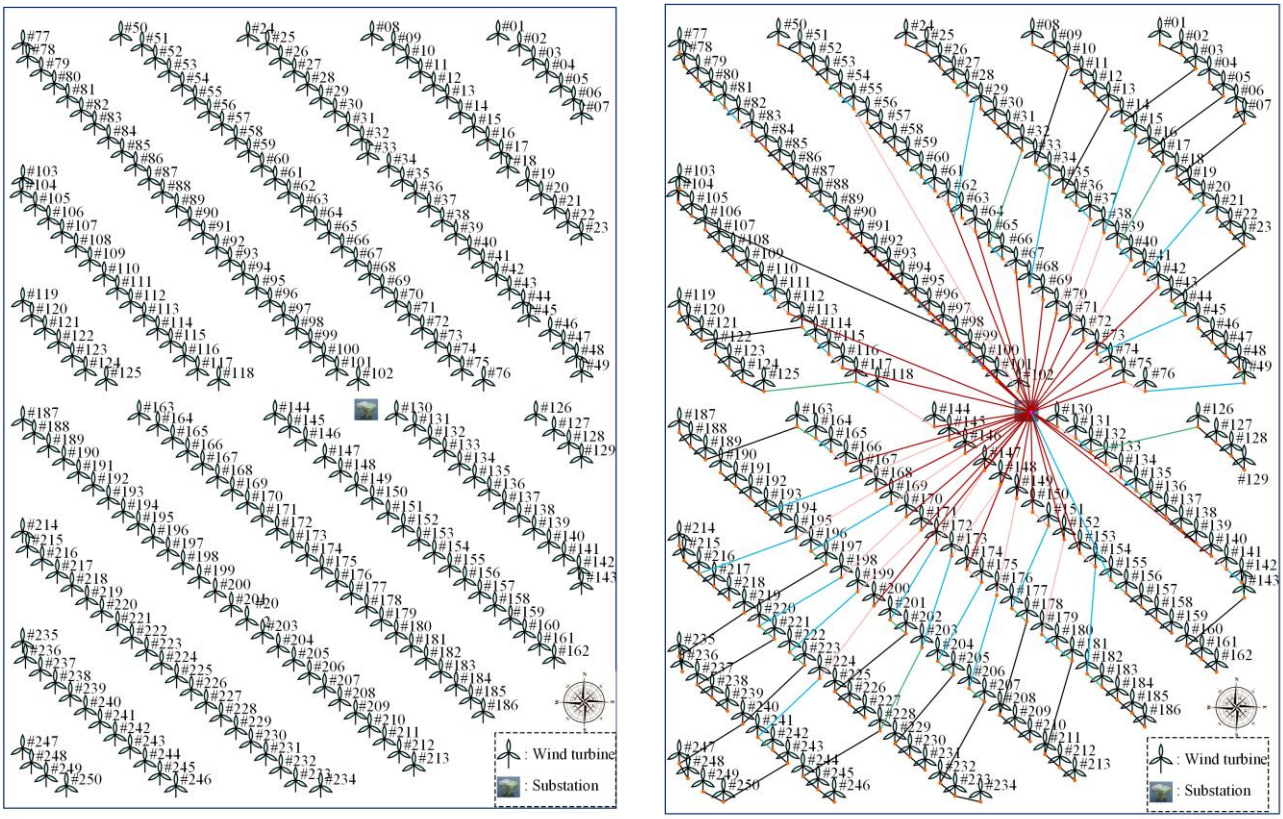

(a) (b)

Fig. 13. The wind turbine connection graphs obtained by ISA for optimal design of CST in test system #2. (a) OWF layout. (b) ISA.

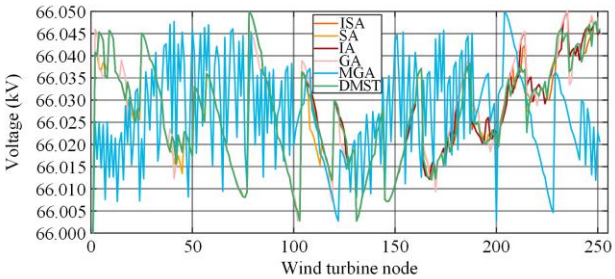

Fig. 14. The wind turbine node voltage of different algorithms for optimal design of CST in test system #2.

V. CONCLUSION

In this paper, a new hybrid method based on graph theory, meta-heuristic optimization, and a grouping-based method is proposed for the optimal design of a CST for a large-scale OWF. The main conclusions:

1) The proposed grouping-based method can dramatically reduce the optimization complexity and difficulty. The graph theory-based improved DMST can significantly enhance the local topology quality for each WT group, while a high optimization efficiency

can be guaranteed. The proposed ISA can effectively avoid trapping into low-quality solutions for the CST via a wide global exploration for different WT groups. Consequently, the proposed method can not only acquire high-quality solutions for CST, but also guarantee optimization stability and efficiency.

2) Comprehensive case studies with two test systems are conducted to demonstrate the effectiveness and advantages of the proposed method, in which four meta-heuristic algorithms and a deterministic algorithm are adopted for comparison. The simulation results confirm that the proposed method can achieve lower capital costs for all the test systems, in which the cost reduction ranges from 0.163% to 0.921% against the comparative methods. Also, the computation cost for optimal design of the CST can be reduced from between 92.329% to 97.668% between the proposed method and other methods. The variation of optimization results using the proposed method is slightly larger than the deterministic algorithm.

APPENDIX A

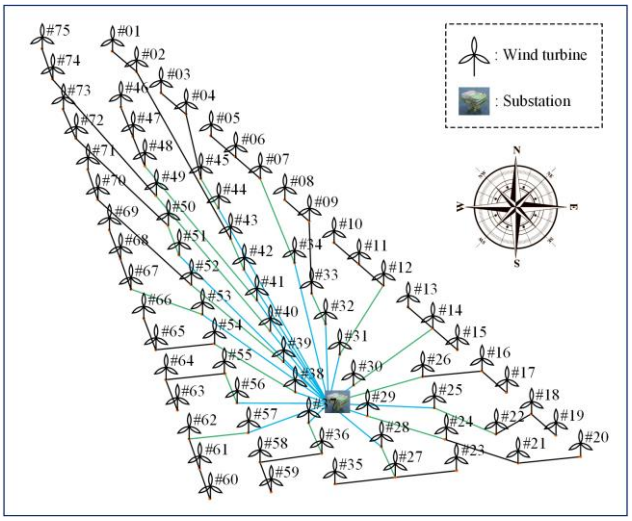

Fig. A1. The wind turbine connection graphs obtained by SA for optimal design of CST in test system #1.

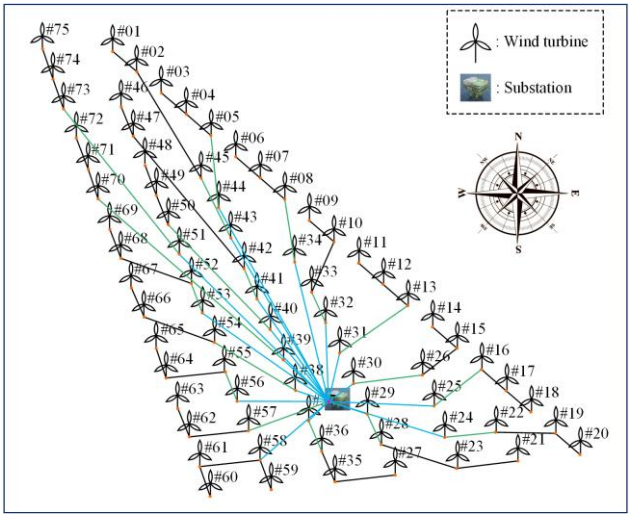

Fig. A2. The wind turbine connection graphs obtained by IA for optimal design of CST in test system #1.

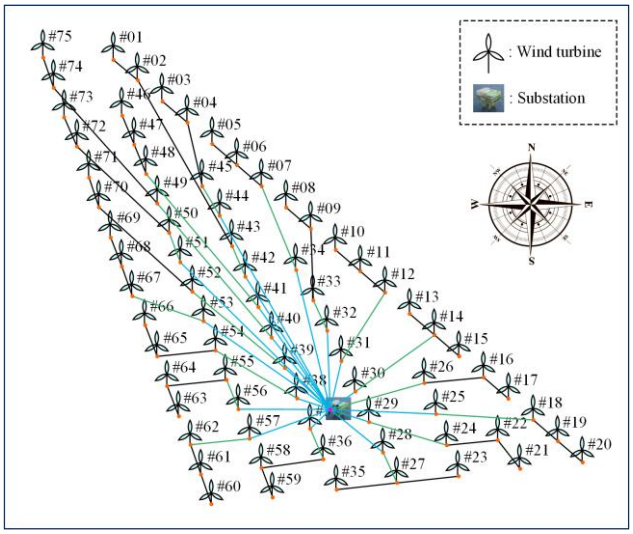

Fig. A3. The wind turbine connection graphs obtained by GA for optimal design of CST in test system #1.

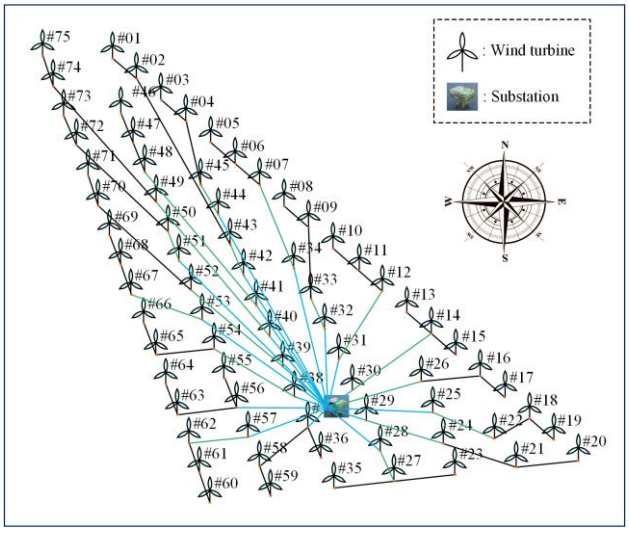

Fig. A4. The wind turbine connection graphs obtained by MGA for optimal design of CST in test system #1.

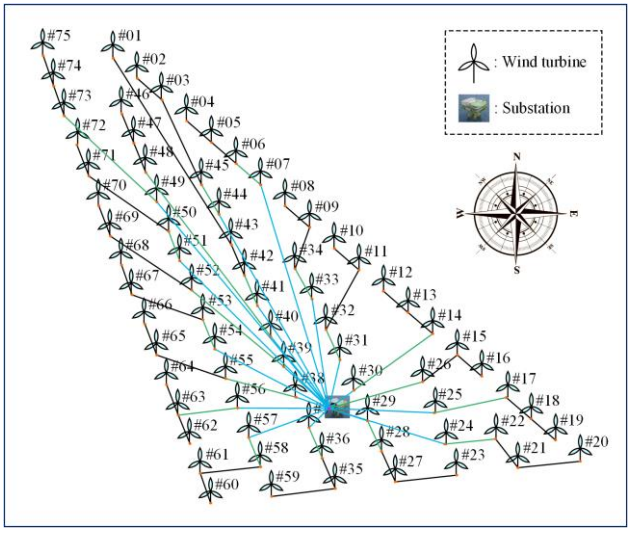

Fig. A5. The wind turbine connection graphs obtained by DMST for optimal design of CST in test system #1.

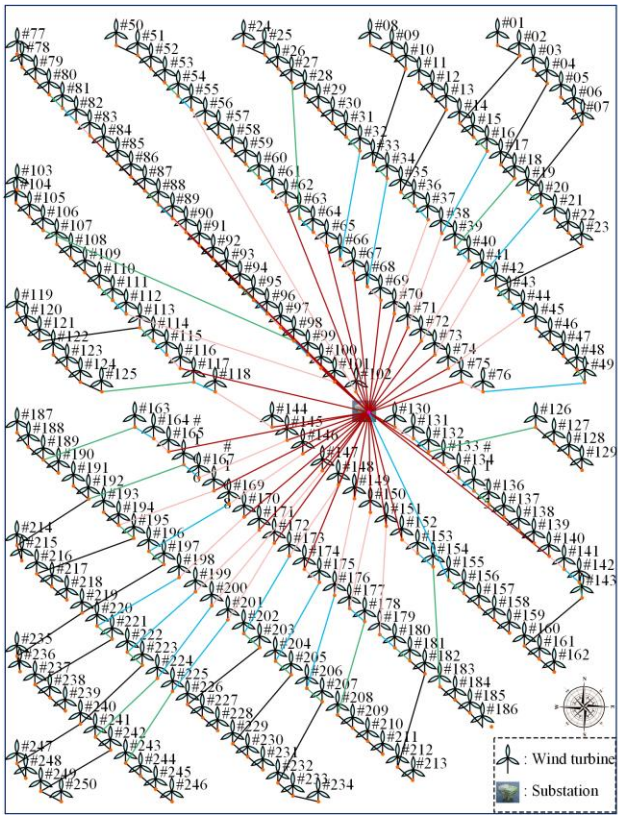

Fig. A6. The wind turbine connection graphs obtained by SA for optimal design of CST in test system #2.

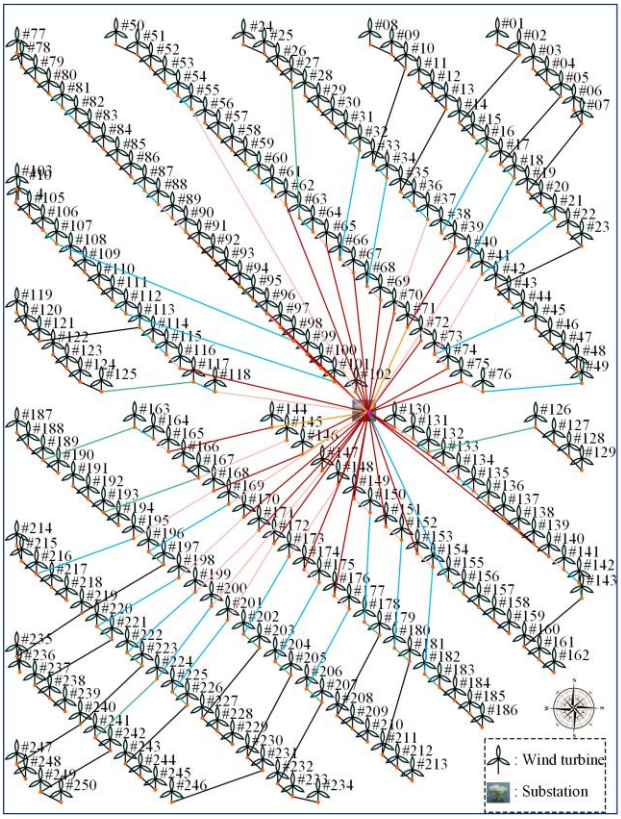

Fig. A8. The wind turbine connection graphs obtained by GA for optimal design of CST in test system #2.

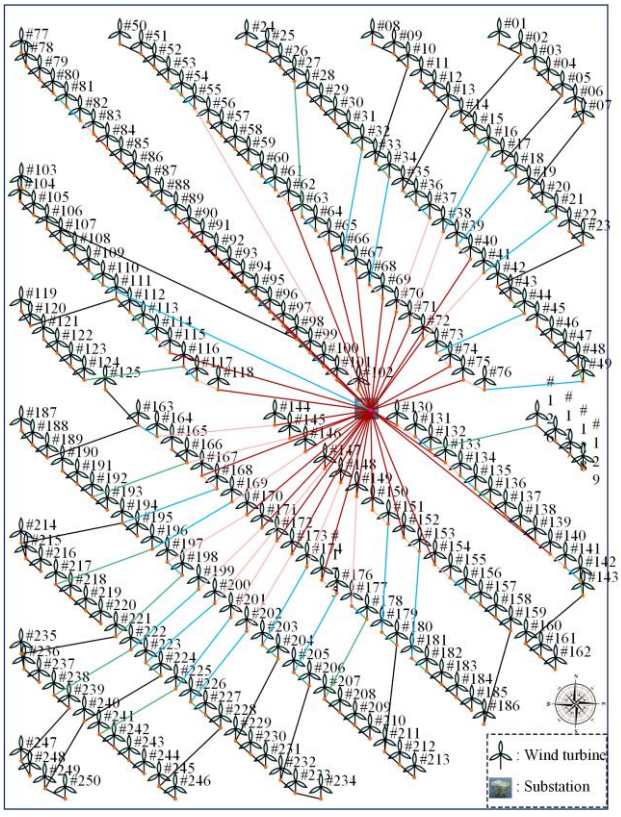

Fig. A7. The wind turbine connection graphs obtained by IA for optimal design of CST in test system #2.

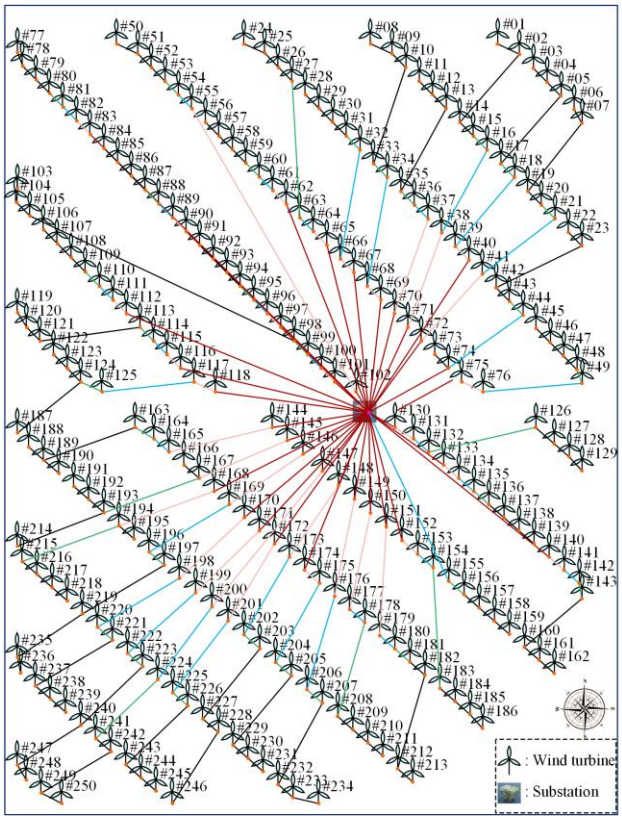

Fig. A9. The wind turbine connection graphs obtained by MGA for optimal design of CST in test system #2.

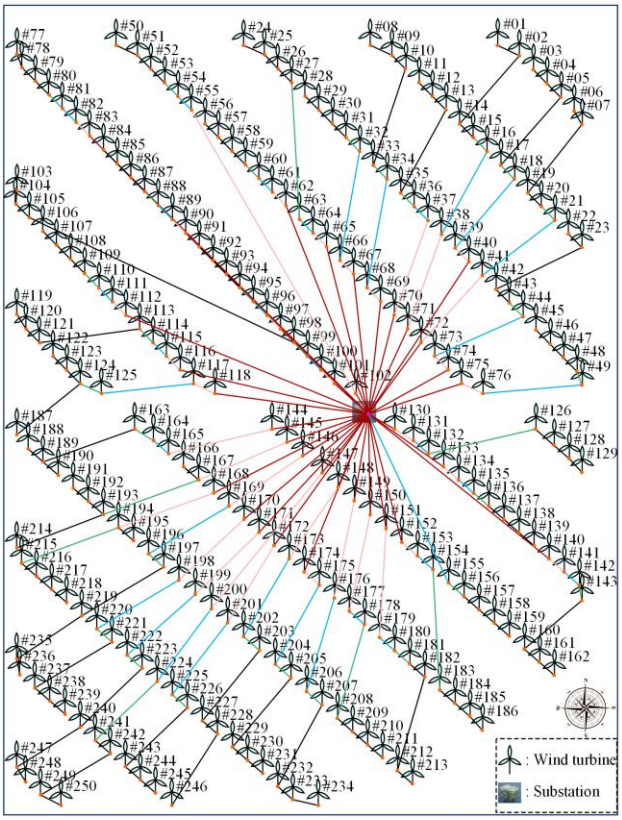

Fig. A10. The wind turbine connection graphs obtained by DMST for optimal design of CST in test system #2.

ACKNOWLEDGMENT

Not applicable.

AUTHORS' CONTRIBUTIONS

Ruilin Chen: software, visualization writing, original draft preparation. Zeyu Zhang: supervision, data sharing. Junxuan Hu: investigation, validation. Lei Zhao: supervision, conceptualization. Chuangzhi Li: methodology, writing, software. Xiaoshun Zhang: methodology, writing, reviewing and editing. All authors read and approved the final manuscript.

FUNDING

This work is jointly supported by the National Key Research and Development Program of China (No. 2022YFF0606600), and the Fundamental Research Funds for the Central Universities (No. N2229001).

AVAILABILITY OF DATA AND MATERIALS

Not applicable.

DECLARATIONS

Competing interests: The authors declare that they have no known competing financial interests or personal relationships that could have appeared to influence the work reported in this article.

AUTHORS' INFORMATION

Ruilin Chen received the B.S. degree from the Guangdong Ocean university, Zhanjiang, China, in 2021. He is currently working toward the M.S. degree in smart grids with Shantou University, Shantou, China. He current research interests include wind power and carbon emission metering.

Zeyu Zhang received the B.S. and M.S. degrees in electrical engineering from South China University of Technology, in 2016. He has been an electrical engineer with ZHONGNAN ENGINEERING CORPORATION LIMITED since 2016. His research interests include artificial intelligence and smart grid, new energy power generation control and operation.

Junxuan Hu received the B.S. and M.S. degrees in electrical engineering from Central South University, in 2011. He has been an electrical engineer at ZHONGNAN ENGINEERING CORPORATION LIMITED since 2011, and has been pursuing a Ph.D. degree in clean energy technology at North China Electric Power University since 2022.His research interests include artificial intelligence and smart grid, new energy power generation control and operation.

Lei Zhao received the B.S., M.S., and Ph.D. degrees in electrical engineering from the Harbin Institute of Technology, Harbin, China, in 2011, 2013, and 2018, respectively. He is currently an associate professor with the Department of Electronic and Information Engineering, College of Engineering, ShantouUniversity, Shantou, China. His research interests include power conversion and control technology.

Chuangzhi Li received the B.Eng. degree in electrical engineering from Guangdong University of Technology, Guangzhou, China, in 2020. Now, he is currently pursuing the Ph.D. degree in the Sichuan university, Chengdu, China. His major research interests include automatic generation control and machine learning application in power engineering.

Xiaoshun Zhang received the Ph.D. degree in the College of Electric Power, South University of Technology, China, in 2017. Dr. Zhang is currently an Associate Professor with the Foshan Graduate School of Innovation, Northeastern University, Foshan, China. His research interests include artificial intelligence based new power system operation and control.

REFERENCES

[1] M. Fischetti and D. Pisinger, "Mixed integer linear programming for new trends in wind farm cable routing," *Electronic Notes in Discrete Mathematics*, vol. 64, pp. 115-124, Feb. 2018.

[2] Global Wind Energy Council, "Global wind report 2022," [Online]. Available:https:/gwec.net/global-wind-report-2022/

[3] "Offshore wind market report: 2021 Edition, energy efficiency and renewable energy," [Online]. Available: https://www.energy.gov/eere/wind/articles/offshore-wind-market-report-2021-edition-released

[4] "Offshore wind market report: 2022 Edition, energy efficiency and renewable energy," [Online]. Available: https://www.energy.gov/eere/wind/articles/offshore-wind-market-report-2022-edition

[5] G. Li, Y. Xu, and S. Jiang *et al*., " Coordinated control strategy for receiving-end AC fault ride-through of an MMC-HVDC connecting offshore wind power," *Power System Protection and Control*, vol. 50, no. 07, pp. 111-119, Apr. 2022. (in Chinese)

[6] M. Zhao, Z. Chen, and F. Blaabjerg, "Optimisation of electrical system for offshore wind farms via genetic algorithm," *IET Renewable Power Generation*, vol. 3, no. 2, pp. 205-216, Jul. 2009.

[7] B. Li, D. Zheng, and B. Li *et al*., "Analysis of low voltage ride-through capability and optimal control strategy of doubly-fed wind farms under symmetrical fault," *Power System Protection and Control*, vol. 8, no. 2, pp. 585-599, Apr. 2023.

[8] M. Fischetti and D. Pisinger, "Optimizing wind farm cable routing considering power losses," *European Journal of Operational Research*, vol. 270, no. 3, pp. 917-930, Nov. 2018.

[9] C. El Mokhi and A. Addaim, "Optimal substation location of a wind farm using different metaheuristic algorithms," in *2020 IEEE 6th International Conference on Optimization and Applications (ICOA)*, Beni Mellal, Morocco, May 2020, pp. 1-6.

[10] R.B. Damala, R.K. Patnaik, and A.R. Dash, "A simple decision tree-based disturbance monitoring system for VSC-based HVDC transmission link integrating a DFIG wind farm," *Protection and Control of Modern Power Systems*, vol. 7, no. 2, pp. 363-381, Apr. 2022.

[11] D. Li, C. He, and H. Shu, "Optimization of electric distribution system of large offshore wind farm with improved genetic algorithm," in *2008 IEEE Power and Energy Society,* Pittsburgh, USA, Jul. 2008, pp. 1-6.

[12] J. S. Gonz´alez, M. B. Pay´an, and J. R. Santos, "A new and efficient method for optimal design of large offshore wind power plants," *IEEE Transactions on Power Systems*, vol. 28, no. 3, pp. 3075-3084, Apr. 2013.

[13] F. M. Gonzalez-Longatt, P. Wall, and P. Regulski *et al*., "Optimal electric network design for a large offshore wind farm based on a modified genetic algorithm approach," *IEEE Systems Journal*, vol. 6, no. 1, pp. 164-172, Sep. 2011.

[14] O. Dahmani, S. Bourguet, and M. Machmoum *et al*., "Optimization of the connection topology of an offshore wind farm network," *IEEE Systems Journal*, vol. 9, no. 4, pp. 1519-1528, Aug. 2014.

[15] Y. Zhang, Y. Qiao, and Z. Lu *et al*., "Optimisation of offshore wind farm collection systems-based on modified genetic algorithm," *The Journal of Engineering*, vol. 2017, no. 13, pp. 1045-1049, Jan. 2018.

[16] D. Li, C. He, and Y. Fu, "Optimization of internal electric connection system of large offshore wind farm with hybrid genetic and immune algorithm," in *2008 Third International Conference on Electric Utility Deregulation and Restructuring and Power Technologies*, Nanjing, China, May 2008, pp. 2476-2481.

[17] P. Hou, G. Yang, and W. Hu *et al*., "Cable connection scheme optimization for offshore wind farm considering wake effect," in *2018 IEEE Congress on Evolutionary Computation (CEC)*, Rio de Janeiro, Brazil, Jul. 2018, pp. 1-8.

[18] S. Tao, Q. Xu, A. Feij´oo, and G. Zheng, "Joint optimization of wind turbine micrositing and cabling in an offshore wind farm," *IEEE Transactions on Smart Grid*, vol. 12, no. 1, pp. 834-844, Sep. 2020.

[19] P. Hou, W. Hu, and Z. Chen, "Optimisation for offshore wind farm cable connection layout using adaptive particle swarm optimisation minimum spanning tree method," *IET Renewable Power Generation*, vol. 10, no. 5, pp. 694-702, May 2016.

[20] R. Srikakulapu and U. Vinatha, "Optimal design of collector topology for offshore wind farm based on ant colony optimization approach," in *2016 IEEE International Conference on Power Electronics, Drives and Energy Systems (PEDES)*, Trivandrum, India, May 2016, pp. 1-6.

[21] B. C. Neagu and G. Georgescu, "Wind farm cable route optimization using a simple approach," in *2014 International Conference and Exposition on Electrical and Power Engineering (EPE)*, Iasi, Romania, Dec. 2014, pp. 1004-1009.

[22] L. Huang, N. Chen, and H. Zhang *et al*., "Optimization of large scale offshore wind farm electrical collection systems based on improved FCM," in *International Conference on Sustainable Power Generation and Supply (SUPERGEN 2012)*, Hangzhou, China, Apr. 2012, pp. 1-6.

[23] T. Zuo, K. Meng, and Z. Tong *et al*., "Offshore wind farm collector system layout optimization based on self-tracking minimum spanning tree," *International Transactions on Electrical Energy Systems*, vol. 29, no. 2, Feb. 2019.

[24] Y. Chen, Z. Dong, and K. Meng *et al*., "A novel technique for the optimal design of offshore wind farm electrical layout," *Journal of Modern Power Systems and Clean Energy*, vol. 1, no. 3, pp. 254-259, Dec. 2013.

[25] P. Hou, W. Hu, and Z. Chen, "Offshore wind farm cable connection configuration optimization using dynamic minimum spanning tree algorithm," in *2015 50th International Universities Power Engineering Conference (UPEC)*, Stoke on Trent, UK, Sep. 2015, 1-6.

[26] T. Zuo, Y. Zhang, and K. Meng, "Collector system topology for large-scale offshore wind farms considering cross-substation incorporation," *IEEE Transactions on Sustainable Energy*, vol. 11, no. 3, pp. 1601-1611, Aug. 2019.

[27] S. Dutta and T. J. Overbye, "Optimal wind farm collector system topology design considering total trenching length," *IEEE Transactions on Sustainable Energy*, vol. 3, no. 3, pp. 339-348, Apr. 2012.

[28] C. El Mokhi and A. Addaim, "Optimal design of the cable layout in offshore wind farms using firefly algorithm and minimum spanning tree," in *2021 7th Inter-*

national Conference on Optimization and Applications (ICOA), Wolfenbüttel, Germany, May 2021, pp. 1-5.

[29] J. S. Shin, W. W. Kim, and J. O. Kim, "Study on designing for inner grid of offshore wind farm," *Journal of Clean Energy Technologies*, vol. 3, no. 4, pp. 265-269, Jan. 2015.

[30] S. Wei, L. Zhang, and Y. Xu *et al*., "Hierarchical optimization for the double-sided ring structure of the collector system planning of large offshore wind farms," *IEEE Transactions on Sustainable Energy*, vol. 8, no. 3, pp. 1029-1039, Dec. 2016.

[31] T. Zuo, Y. Zhang, and K. Meng, "Double-sided ring topology for offshore wind farm collector system layout: a multi-cable application," in *8th Renewable Power Generation Conference (RPG 2019)*, Shanghai, China, Oct. 2019.

[32] T. Zuo, Y. Zhang, and K. Meng *et al*., "A two-layer hybrid optimization approach for large-scale offshore wind farm collector system planning," *IEEE Transactions on Industrial Informatics*, vol. 17, no. 11, pp. 7433-7444, Feb. 2021.

[33] B. Yang, B. Liu, and H. Zhou *et al*., "A critical survey of technologies of large offshore wind farm integration: summary, advances, and perspectives," *Protection and Control of Modern Power Systems*, vol. 7, no. 2, pp. 233-264, Apr. 2022.

[34] H. Laghridat, A. Essadki, and T. Nasser, "Coordinated control by ADRC strategy for a wind farm based on SCIG considering low voltage ride-through capability," *Protection and Control of Modern Power Systems*, vol. 7, no. 1, pp. 82-99, Jan. 2022.

[35] L. Huang and Y. Fu, "Reliability evaluation of the offshore wind farm," in *2010 Asia-Pacific Power and Energy Engineering Conference*, Chengdu, China, Apr. 2010, pp. 1-5.

[36] E. Spahic, A. Underbrink, and V. Buchert *et al*., "Reliability model of large offshore wind farms," in *2009 IEEE Bucharest PowerTech*, Bucharest, Romania, Oct. 2009, pp. 1-6.

[37] O. Dahmani, S. Bourguet, and M. Machmoum *et al*., "Reliability analysis of the collection system of an offshore wind farm," in *2014 Ninth International Conference on Ecological Vehicles and Renewable Energies (EVER)*, Monte-Carlo, Monaco, Jun. 2014, pp. 1-6.

[38] D. Petkovic´, S. Shamshirband, and N. Anuar *et al*., "An appraisal of wind speed distribution prediction by soft computing methodologies: a comparative study," *Energy conversion and Management*, vol. 84, pp. 133-139, Aug. 2014.

[39] Thorne & Derrick, "Wind power plants internal distribution system and grid connection: A technical and economical comparison between a 33 kV and a 66 kV," [Online]. Available: https://www.powerandcables.com/wp-content/uploads/2019/03/33kV-v-66kV-A-Wind-Farm-Collection-Grid-Technical-Comparison/